




A comparison of solution and solid state coordination environments for calcium(II), zirconium(IV), cadmium(II) and mercury(II) complexes with dipicolinic acid and methylimidazole derivatives

Mohammad Ghadermazi, Zohreh Derikvand, Zahra Mahmoudiazar, Elham Shahnejat, Hadi Amiri Rudbari, Giuseppe Bruno, Ardeshir Shokrollahi, Sara Nasiri & Parisa Mehdizadeh Naderi

To cite this article: Mohammad Ghadermazi, Zohreh Derikvand, Zahra Mahmoudiazar, Elham Shahnejat, Hadi Amiri Rudbari, Giuseppe Bruno, Ardeshir Shokrollahi, Sara Nasiri & Parisa Mehdizadeh Naderi (2015) A comparison of solution and solid state coordination environments for calcium(II), zirconium(IV), cadmium(II) and mercury(II) complexes with dipicolinic acid and methylimidazole derivatives, *Journal of Coordination Chemistry*, 68:22, 3982-4002, DOI: [10.1080/00958972.2015.1079627](https://doi.org/10.1080/00958972.2015.1079627)


To link to this article: <http://dx.doi.org/10.1080/00958972.2015.1079627>

 View supplementary material 

 Accepted author version posted online: 10 Aug 2015.
Published online: 25 Aug 2015.

 Submit your article to this journal 

 Article views: 96

 View related articles 

 View Crossmark data 

A comparison of solution and solid state coordination environments for calcium(II), zirconium(IV), cadmium(II) and mercury(II) complexes with dipicolinic acid and methylimidazole derivatives

MOHAMMAD GHADERMAZI*[†], ZOHREH DERIKVAND[‡],
ZAHRA MAHMOUDIAZAR[†], ELHAM SHAHNEJAT[†], HADI AMIRI RUDBARI[§],
GIUSEPPE BRUNO[¶], ARDESHIR SHOKROLLAHI^{††}, SARA NASIRI^{||} and
PARISA MEHDIZADEH NADERI^{||}

[†]Department of Chemistry, Faculty of Science, University of Kurdistan, Sanandaj, Iran

[‡]Department of Chemistry, Faculty of Science, Khorramabad Branch, Islamic Azad University, Khorramabad, Iran

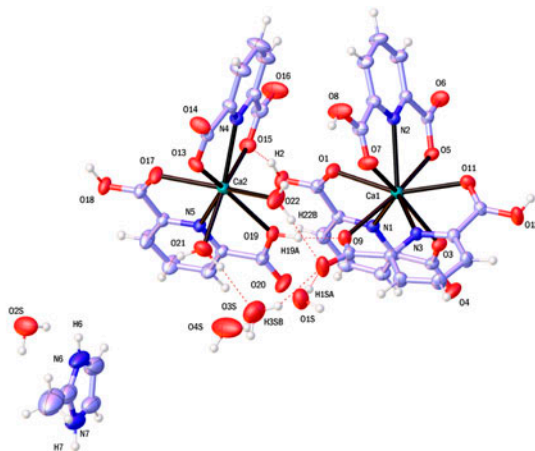
[§]Department of Chemistry, University of Isfahan, Isfahan, Iran

[¶]Department of Chemical Sciences, University of Messina, Messina, Italy

^{||}Department of Chemistry, Yasouj University, Yasouj, Iran

^{††}Radiation and Pollution Protection Research Center of Mamasani, Mamasani, Iran

(Received 8 July 2014; accepted 16 July 2015)



Four new supramolecular compounds, (2-mimH)[Ca(pydcH)₃][Ca(pydcH₂)(pydc)(H₂O)₂]·4H₂O (**1**), (1-mimH)₂[Zr(pydc)₃] (**2**), (2-mimH)₂[Cd(pydc)₂]·8H₂O (**3**), and (2-mimH)₂[Hg(pydc)₂]·8H₂O (**4**) [where pydcH₂ = pyridine-2,6-dicarboxylic acid (dipicolinic acid), 1-mim = 1-methylimidazole, and 2-mim = 2-methylimidazole], have been synthesized and characterized by elemental analyses, spectroscopic techniques (IR, UV–vis, ¹H NMR, and ¹³C NMR), thermal (TG/DTG/DTA) analysis as

*Corresponding author. Email: mghadermazi@uok.ac.ir

well as single-crystal X-ray diffraction. All four compounds are proton-transfer salts of the methylimidazolium cations and metal complex anions that crystallized from a solution of pyridine-2,6-dicarboxylic acid, methylimidazole, metal nitrates or chlorides as starting materials. The coordinating dicarboxylic acid is deprotonated at the carboxyl group and methylimidazole is protonated to balance the charge. In the crystal structures of **1–4**, hydrogen bonding and π - π stacking play important roles. Water clusters are formed in **1**, **3**, and **4**. The equilibrium constants of dipicolinic acid (pydc) and methylimidazole derivatives (1-mim and 2-mim), pydc-2-mim, pydc-1-mim proton-transfer systems as well as those of their complexes were investigated by a potentiometric pH titration method. The stoichiometries of most of the complex species in solution were very similar to the cited crystalline metal ion complexes.

Keywords: Solution studies; Methylimidazole; Nine- and eight-coordinated Ca(II); Crystal structure

1. Introduction

The complexation of metal ions with dipicolinic acid has attracted interest owing to its ability to form stable chelates with a diversity of configurations and plentiful structural motifs. Dipicolinic acid can stabilize remarkable oxidation states of transition metals and can be used in analytical chemistry [1–3]. This ligand has attracted much interest in coordination chemistry because of its low toxicity and amphiphilic nature [4]. Compared with other pyridine dicarboxylic acids, pyridine-2,6-dicarboxylic acid (H₂pydc) has merits over the former with richer coordination modes, hydrogen bond donors and acceptors [5–7]. The O–H···O, N–H···O, and N–H···N hydrogen bonds have the strong directional effect to organize individual molecules into supramolecular architectures as ribbons, rosettes, layers, tubes, rods, spheres, and sheets. Pyridine-2,6-dicarboxylic acid is therefore regarded as a candidate for construction of metal organic polymers [8–10(b)]. The nitrogen of the aromatic ring between two carboxylic acid groups allows dipicolinate anion to behave as a tridentate ligand; it forms dianionic complexes. The pydcH₂ is suitable for designing coordination compounds with various dimensionalities and inducing self-assembly processes. In continuation of our research on the synthesis of transition metals and main group complexes with polycarboxylate ligands in the presence of some amino compounds, we became interested in studies of metal complexes with methylimidazole derivatives as secondary ligands. We used pydcH₂ as an excellent candidate for constructing heterobimetallic coordination polymers. Our research group has published two heterobimetallic coordination polymers of pydcH₂ with zinc, nickel, and calcium [10(c)]. In addition, other complexes of this ligand with various amines have been reported [10(c)–(f)]. In all of these complexes, hydrogen bonding plays an important role in the stability of crystal structures. The various components of those complexes tightly connect to each other *via* intermolecular hydrogen bonding. We become fascinated in the study of metal complexes with imidazole derivatives (1-methylimidazole and 2-methylimidazole). Derivatives of imidazole as heterocyclic compounds were used to construct coordination compounds. Imidazole derivatives [10(g), (h)] are present in important biological building blocks, such as histidine, and the related hormone histamine, also various drugs contain an imidazole ring, for instance, antifungal drugs, nitroimidazole, and the sedative midazolam [10(i), (j)]. Moreover, imidazole derivatives are excellent proton acceptor ligands and facilitate proton-transfer processes, supporting formation of complexes.

Here, we describe the synthesis, spectroscopic, elemental, and thermal analysis, crystal structures, and solution studies of pydcH₂ complexes with methylimidazole derivatives

(1-mim and 2-mim), (2-mimH)[Ca(pydcH)₃][Ca(pydcH₂)(pydc)(H₂O)₂] \cdot 4H₂O (**1**), (1-mimH)₂[Zr(pydc)₃] (**2**), (2-mimH)₂[Cd(pydc)₂] \cdot 8H₂O (**3**), and (2-mimH)₂[Hg(pydc)₂] \cdot 8H₂O (**4**). The four compounds consist of anionic metal complexes with protonated methylimidazole derivatives as counter cations. There are neutral (pydcH₂), monoanionic (pydcH⁻), and dianionic (pydc²⁻) forms of pyridine-2,6-dicarboxylic acid in **1** which connected simultaneously to calcium. The presence of neutral, monoanionic, and dianionic forms of this ligand in one complex is quite rare. Surprisingly, **1** is a co-crystal compound since two different Ca(II) complexes with different coordination geometry are crystallized simultaneously. Water clusters occur in crystals of **1**, **3**, and **4**. All the components in **1**–**4** are strongly associated to each other *via* a complex arrangement of hydrogen bonds, electrostatic interactions, and $\pi\cdots\pi$ stacking.

2. Experimental

2.1. General methods and materials

All materials were purchased from Merck. Solvents used throughout the reactions were of high purity. IR spectroscopy was performed on a Bruker Vector 22 FT-IR spectrophotometer from 4000 to 400 cm⁻¹ using KBr pellets. The UV–vis spectra of the complexes were recorded on a Cary Varian E100 UV–vis spectrophotometer from 200–900 nm at room temperature. ¹H NMR spectra were taken on a Bruker 250 MHz spectrometer. Chemical shifts are reported on the δ scale relative to TMS. Elemental analysis was performed with a Perkin–Elmer 2004(II) apparatus. The X-ray data were obtained with a Bruker SMART ApexII diffractometer. Potentiometric titrations were carried out with a Model 794 Metrohm Basic Titrino that was attached to an extension combined glass-calomel electrode mounted in an air-protected, sealed, thermostated jacketed cell maintained at 25.0 \pm 0.1 $^{\circ}$ C by circulating water, from a constant-temperature bath Fisherbrand model FBH604, LAUDA, Germany, equipped with a stirrer and a 10.000-mL-capacity Metrohm piston buret. The pH meter–electrode system was calibrated to read $-\log [H^+]$. Thermal analyses (TG–DTG) including the thermogravimetry (TG) and derivative thermogravimetry (DTG) were carried out using a PL-1500 TGA and Perkin–Elmer Thermal Analysis with heating rate of 10 $^{\circ}$ C min⁻¹ in N₂ atmosphere.

2.2. Synthesis of (2-mimH)[Ca(pydcH)₃][Ca(pydcH₂)(pydc)(H₂O)₂] \cdot 4H₂O (**1**)

A solution of 2-methylimidazole (164 mg, 2 mmol) in THF (10 mL) was added to a solution of pyridine-2,6-dicarboxylic acid (167 mg, 1 mmol) in THF (500 mL) under stirring in a 2 : 1 molar ratio. The solution was heated to 70 $^{\circ}$ C. When the solution was cooled in water, a white product was obtained. The resulting solid was filtered off and dried at room temperature (95% yield for C₁₅H₁₇N₅O₄). ¹H NMR (D₂O): H 2.53 ppm (m, 6H, 2CH₃), H 7.21 ppm (m, 2H, 2(2-mimH)⁺), H 8.25 ppm (m, 2H, 2(2-mimH)⁺), H 8.30 (m, 3H, pydc²⁻). Then, this compound (165 mg, 0.5 mmol) and CaCl₂ (28 mg, 0.25 mmol) were dissolved in distilled water (15 mL) at pH 6 and stirred for 15 min at room temperature. The mother liquid was kept at room temperature until colorless crystals of **1** suitable for X-ray diffraction were obtained after 20 days. The crystals were collected in 86% yield. M.p 204 $^{\circ}$ C. *Anal.* Calcd for C₃₉H₃₉Ca₂N₇O₂₆: C, 42.51; H, 3.57; N, 8.90%. Found: C,

41.99; H, 3.48; N, 8.88%. IR (KBr disk, ν (cm⁻¹)): 3400br, 3123w, 2918w, 2710w, 1748s, 1620s, 1571s, 1431s, 1359s, 1322s, 1271s, 1189s, 1069m, 1010m, 879s, 767s, 655s. ¹H NMR (D₂O): H 2.40 ppm (s, 3H, CH₃), H 7.08 ppm (s, 2H, (2-mimH)⁺), H 8.05 (t, H, pydc²⁻), H 8.20 (t, 2H, pydc²⁻). ¹³C NMR (D₂O): C 10.3 ppm (CH₃, 2-mimH⁺), C 118 ppm (C_{meta}, pydc²⁻), C 126.4 ppm (C_{para}, pydc²⁻), C 142.9 ppm (C_{ortho}, pydc²⁻), C 144 ppm (C2, 2-mimH⁺), C 148.3 ppm (C1, 2-mimH⁺), 168.4 ppm (CO, pydc²⁻), UV-vis (aqueous solution) (λ , nm): 215, 260.

2.3. Synthesis of (1-mimH)₂[Zr(pydc)₃] (2)

A solution of 1-methylimidazole (1 mL, 6 mmol) was added to a solution of pyridine-2,6-dicarboxylic acid (501 mg, 3 mmol) in THF (500 mL) under stirring in a 2 : 1 molar ratio. The solution was heated to 70 °C. When the solution was cooled in water, a white solid was obtained. The resulting solid was filtered off and dried at room temperature (92% yield for C₁₅H₁₇N₅O₄), ¹H NMR (D₂O): H 2.49 ppm (s, 6H, 2CH₃), H 7.15 ppm (s, 2H, 2 (1-mimH)⁺), H 8.24–8.26 (d, 4H, 2(1-mimH)⁺), H 8.41–8.47 ppm (t, 3H, (pydc²⁻)). Then, this compound (165 mg, 0.5 mmol) and ZrOCl₂·8H₂O (80 mg, 0.25 mmol) were dissolved in distilled water (15 mL) at pH 5.5 and stirred for 15 min at room temperature. Colorless crystals, suitable for X-ray analysis, were obtained by slow evaporation of the solvent at room temperature. The crystals were collected in 53% yield. M.p. > 340 °C. Anal. Calcd for C₂₉H₂₃N₇O₁₂Zr: C, 46.2; H, 3.05; N, 13.01%. Found: C, 45.8; H, 3.1; N, 13.1%. IR (KBr disk, ν (cm⁻¹)): 3130s, 1640s, 1477s, 1435s, 1386s, sh, 1273s, 1187s, 1141s, 1074s, 1030s, 920s, 740s, 683s, 631s. ¹H NMR (D₂O): H 3.79 ppm (s, 6H, 2CH₃), H 7.30 ppm (s, 2H, 1-mimH⁺), H 8.06 (d, 4H, 1-mimH⁺), H 8.27 (t, 6H, pydc²⁻), H 8.52 (s, 3H, pydc²⁻) (figure 1S). ¹³C NMR (D₂O): C 9.85 ppm (CH₃, 1-mimH⁺), C 117.5 ppm (C_{meta}, pydc²⁻), 125.8–126.6 ppm (C_{para}, pydc²⁻), C 143.5–143.9 ppm (C_{ortho}, pydc²⁻ and C 1-mimH⁺), C 147 ppm (C1, 1-mimH⁺), C 165.92 ppm (CO, pydc²⁻), UV-vis (aqueous solution) (λ , nm): 274, 282.

2.4. Synthesis of (2-mimH)₂[Cd(pydc)₂]·8H₂O (3)

Compound **3** was prepared at pH 7 in a parallel approach as described for **1**, except that CaCl₂ was replaced by Cd(NO₃)₂·4H₂O. Colorless crystals, suitable for X-ray analysis, were obtained by slow evaporation of the solvent at room temperature. The crystals were collected in 63% yield. M.p. 170 °C. Anal. Calcd for C₂₂H₃₆CdN₆O₁₆: C, 35.08; H, 4.8; N, 11.6%. Found: C, 35.28; H, 4.8; N, 11.20%. IR (KBr disk, ν (cm⁻¹)): 3407–33,128 br, 2941br, m, 1692s, 1618s, 1570s, 1426s, 1375s, 1275s, 1164s, 888s, 791s, 728s. ¹H NMR (D₂O): H 2.47 ppm (s, 3H, CH₃), H 7.14 ppm (s, 2H, 2-mimH⁺), H 8.26–8.56 ppm (m, 3H, pydc²⁻). UV-vis (aqueous solution) (λ , nm): 272, 280.

2.5. Synthesis of (2-mimH)₂[Hg(pydc)₂]·8H₂O (4)

A solution of 2-methylimidazole (1 mL, 6 mmol) was added to a solution of pyridine-2,6-dicarboxylic acid (501 mg, 3 mmol) in THF (500 mL) under stirring in a 2 : 1 molar ratio. The solution was heated to 70 °C. When the solution was cooled in water, a white solid was obtained (95% yield for C₁₅H₁₇N₅O₄). The resulting solid was filtered off and dried at room temperature. Then, this compound (165 mg, 0.5 mmol) and Hg(NO₃)₂

(81 mg, 0.25 mmol) were dissolved in distilled water (15 mL) at pH 5 and stirred for 15 min at room temperature. Colorless crystals, suitable for X-ray analysis, were obtained by slow evaporation of the solvent at room temperature. The crystals were collected in 74% yield. M.p. 316 °C. *Anal.* Calcd for $C_{22}H_{36}HgN_6O_{16}$: C, 31.69; H, 3.36; N, 10.08%. Found: C, 0.81; H, 3.34; N, 9.95%. IR (KBr disk, ν (cm^{-1})): 3108 br, 1732s, 1607s, 11579s, 11445s, 1379s, 11242s, 1177s, 1083s, 1022s, 880s, 760s, 689s. 1H NMR (D_2O): H 2.43 ppm (s, 3H, CH_3), H 7.10 ppm (s, 2H, 2-mimH $^+$), H 8.35–8.53 ppm (m, 3H, pydc $^{2-}$). UV–vis (aqueous solution) (λ , nm): 263.

2.6. Potentiometric measurements

The details are described in previous publications [11–13]. The concentrations of pydc, 2-mim, and 1-mim were 2.5×10^{-3} M for the potentiometric pH titrations of pydc/2-mim and pydc/1-mim in the absence and presence of 1.25×10^{-3} M of Hg^{2+} , Cd^{2+} , and Ca^{2+} ions. In the Zr^{4+} /pydc/1-mim system, although the concentration of ligands is 3.75×10^{-3} M, the Zr^{4+} ion is the same. A standard carbonate-free NaOH solution (0.10016 M) was used in all titrations. The ionic strength was adjusted to 0.1 M with $NaNO_3$ or $NaClO_4$. Before an experimental point (pH) was measured, sufficient time was allowed for the establishment of equilibrium. Distribution diagrams were drawn using the Hyss 2009 program as a new version of it [14]. The protonation constants of ligands and stability constants of proton transfer and their metal complexes were evaluated using the Hyperquad 2008 program [15]. The value of $K_w = [H^+][OH^-]$ is used in the calculations according to our previous work [16].

2.7. Crystal structure determination and refinement

Suitable crystals of **1–4** were selected for X-ray analysis. Single-crystal X-ray diffraction data are collected on a Bruker APEX II equipped with a CCD area detector and utilizing Mo-K α radiation ($\lambda = 0.71073$ Å) at room temperature. Data were collected and reduced by

Table 1. Crystallographic data for **1–4**.

Compound	1	2	3	4
Empirical formula	$C_{39}H_{39}Ca_2N_7O_{26}$	$C_{29}H_{23}N_7O_{12}Zr$	$C_{22}H_{36}CdN_6O_{16}$	$C_{22}H_{36}HgN_6O_{16}$
Formula weight	1101.93	752.76	752	841.16
Crystal system	Triclinic	Monoclinic	Tetragonal	Tetragonal
Space group	$P\bar{1}$	C_2/c	$I41/a$	$I41/a$
a (Å)	11.5693(5)	24.030(7)	9.6663(6)	9.6481(3)
b (Å)	13.0262(6)	10.097(3)	9.6663(3)	9.6481(3)
c (Å)	15.3883(7)	15.549(5)	34.6485(15)	34.6671(15)
α (°)	90.2540(10)	90	90	90
β (°)	94.8900(10)	129.28(2)	90	90
γ (°)	95.8070(10)	90	90	90
Z	2	4	4	4
V (Å 3)	2298.58(18)	2920.4(7)	3237.5(2)	3227.0(2)
D_{calcd} (Mg m $^{-3}$)	1.592	1.712	1.537	1.731
$F(0\ 0\ 0)$	1140	1528	1528	1672
Refl. collected	35,038	85,030	94,183	52,484
No. unique refl.	12,146, $R_{int} = 0.0135$	4705, $R_{int} = 0.021$	2611, $R_{int} = 0.039$	1586, $R_{int} = 0.0416$
Goodness-of-fit on F^2	1.026	1.052	1.135	1.290
R_1 [$I > 2\sigma(I)$]	$R_1 = 0.0358$	0.0243	0.0403	0.0269
wR_2 (all data)	0.1204	0.0712	0.1086	0.0652

SMART and SAINT software in the Bruker packages [17(a)]. The structures were solved by direct methods [17(b)] [SHELXTL.97] and then refined by least squares refinement on F^2 [17(c), (d)]. The complete conditions of data collection and structure are given in table 1. All hydrogens except N–H and O–H were placed in calculated positions and refined as isotropic with the “riding-model technique.” N–H and O–H hydrogens were found in a difference Fourier map and refined isotropically.

3. Results and discussion

3.1. Synthesis and spectroscopic studies

The ion pair compounds were prepared separately by mixing solutions of pyridine-2,6-dicarboxylic acid with 1-methylimidazole or 2-methylimidazole in THF. The two solid products were characterized by ^1H NMR technique (figure 2S). Then, they were applied to synthesize **1–4**. Compounds **1–4** were prepared by similar synthetic procedures. Treatment of $\text{M}(\text{NO}_3)_2$ [$\text{M} = \text{Ca}, \text{Cd}$ or Hg] and ZrOCl_2 with ion pairs containing pyridine-2,6-dicarboxylic acid and methylimidazole derivatives in solution gave **1–4**. Crystals were obtained by gradual cooling and slow evaporation of the solvent at room temperature. Compound **1** appears as rhombic, **2** as prismatic, **3** as colorless needles, and **4** as colorless cubic crystals. Elemental analyses of the complexes are entirely consistent with their determined composition by X-ray crystallography. All the compounds are stable in air and soluble in water. Solution procedure for obtaining crystals is easier and faster than other procedures, such as reflux conditions, hydrothermal methods, and solvothermal procedures.

The IR spectrum of **1** shows a broad band at 3400 cm^{-1} due to $\nu(\text{OH})$ water and pyridine-2,6-dicarboxylic acid. From 2918 to 2710 cm^{-1} $\nu(\text{CH})$ of $(\text{pydc})^{2-}$, $(\text{pydcH})^-$ and pydcH_2 were observed. The IR spectrum of **1** has a band at 1748 cm^{-1} , related to neutral pydcH_2 . The carboxylic groups show strong bands from 1620 to 1571 cm^{-1} . In **1**, these strong bands were shifted and broadened with respect to the corresponding ones in the free dipicolinic acid. The bands at 1621 and 1322 cm^{-1} correspond to the asymmetric and symmetric stretches of carboxyl groups, respectively. The value of $\Delta[\nu_{\text{as}} - \nu_{\text{s}}]$ is 299 cm^{-1} , indicating monochelation of the carboxylic group [17(e)], in agreement with the X-ray crystal analysis. The strong absorptions at 1621 and 1431 cm^{-1} are attributed to the $\nu(\text{C}=\text{C})$ and $\nu(\text{C}=\text{N})$ vibrations in the ligands [18]. Ring wagging vibrations of pyridine groups are also observed at 655 and 765 cm^{-1} . The band at 3123 cm^{-1} is assigned to $\nu(\text{NH})$ of $(2\text{-mimH})^+$.

In **2**, the broad band at 3130 cm^{-1} is attributed to $\nu(\text{NH})$ of $(1\text{-mimH})^+$. The strong absorptions at 1620 and 1385 cm^{-1} correspond to the asymmetric and symmetric stretches of carboxyl groups, respectively. The value of $\Delta[\nu_{\text{as}} - \nu_{\text{s}}]$ is 235 cm^{-1} , indicating monochelation of the carboxylic group. The absorption bands at 1477 and 1436 cm^{-1} may be attributed to $\nu(\text{C}=\text{C})$ and $\nu(\text{C}=\text{N})$ of $(\text{pydc})^{2-}$ anions. These bands are shifted to higher wavenumbers than free ligands, suggesting coordination of pyridyl nitrogen of $(\text{pydc})^{2-}$. IR spectrum of **3** shows a broad band at $3407\text{--}2914\text{ cm}^{-1}$ due to stretching vibrations of OH and NH of water and $(2\text{-mimH})^+$. Strong stretching vibrations at $1692\text{--}1570\text{ cm}^{-1}$ are attributed to single to double CO bonds. The sharp peaks at 1425 and 1375 cm^{-1} are attributed to $\nu(\text{C}=\text{C})$ and $\nu(\text{C}=\text{N})$ of aromatic rings. In the IR spectrum of **4**, a broad band at 3108 cm^{-1} is attributed to vibration of the OH of water and the NH of methylimidazolium. Bands at 1607 and 1379 cm^{-1} correspond to the asymmetric and symmetric stretches of

carboxylates, respectively. The sharp peaks at 1579 and 1445 cm^{-1} are attributed to $\nu(\text{C}=\text{C})$ and $\nu(\text{C}=\text{N})$ of aromatic rings. The electronic spectra of aqueous solutions of **1–4** exhibit some strong absorptions below 300 nm (260 nm) for **1**, 274 and 282 nm for **2**, 272 and 280 nm for **3**, and 263 nm for **4**, which can be assigned to $\pi \rightarrow \pi^*$ and $n \rightarrow \pi^*$ intra-ligand transitions (figures 3S–6S).

3.2. Crystal structures

Compound **1** crystallizes in the triclinic crystal system with $P\bar{1}$ space group. A neutral complex $[\text{Ca}(\text{pydcH}_2)(\text{pydc})(\text{H}_2\text{O})_2]$ is co-crystallized with an anionic complex $(2\text{-mimH})[\text{Ca}(\text{pydcH}_3)]$ in **1** (figure 1). In the crystal structure of **1**, four uncoordinated waters connected the various components. The crystallographic data, bond lengths and angles, and selected intermolecular hydrogen bond parameters are listed in tables 1, 2 and 3, respectively.

We have previously published a coordination polymer of Ca(II) with pyridine-2,6-dicarboxylate [19]. The structure of $([\text{Ca}(\text{pydc})(\mu\text{-H}_2\text{O})(\text{H}_2\text{O})_2]_n)$ is completely different from **1**. In that complex, the $(\text{pydc})^{2-}$ ligands bridge Ca(II) ions and formed a 3D coordination network. Other coordination polymers of this ligand with various metals have been investigated [10(b), (c)] in which $(\text{pydc})^{2-}$ ligands connect metal centers in different coordination modes. The Ca(II) ions in **1** are eight and nine coordinates. In $[\text{Ca}(\text{pydcH}_3)]^-$, three $(\text{pydcH})^-$ are coordinated to Ca(II) in a tridentate chelating fashion through three pyridine nitrogens and six oxygens of carboxylate groups. All Ca–O and Ca–N distances in this anionic complex are different and the sum of bond angles N1–Ca1–N3, N2–Ca1–N3, and

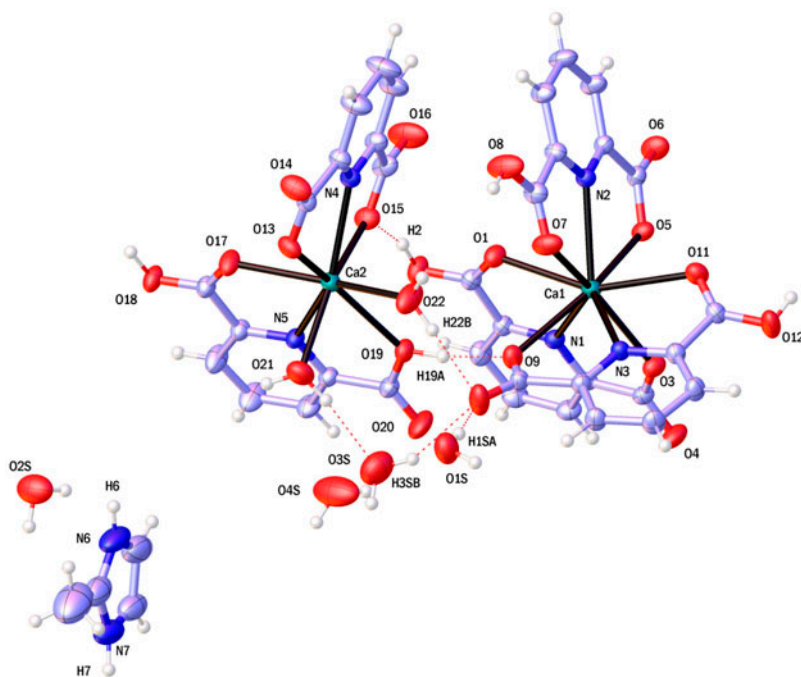


Figure 1. ORTEP diagram of $(2\text{-mimH})[\text{Ca}(\text{pydcH}_3)][\text{Ca}(\text{pydcH}_2)(\text{pydc})(\text{H}_2\text{O})_2] \cdot 4\text{H}_2\text{O}$ (**1**). Non H-atoms represented as displacement ellipsoids are plotted at 50% probability level, while hydrogens are shown as small spheres of arbitrary radius. Water molecules have been omitted for clarity.

Table 2. Selected bond lengths (Å) and angles (°) for 1–4.

<i>Compound 1</i>			
Ca1–O3	2.4494(10)	Ca2–O22	2.3471(13)
Ca1–O5	2.4973(10)	Ca2–O21	2.3923(12)
Ca1–O1	2.5014(11)	Ca2–O17	2.4465(11)
Ca1–N3	2.5236(11)	Ca2–O15	2.4690(11)
Ca1–N1	2.5381(11)	Ca2–O13	2.4785(10)
Ca1–N2	2.5614(11)	Ca2–N4	2.5094(12)
Ca1–O9	2.5665(11)	Ca2–N5	2.5265(11)
Ca1–O11	2.6139(11)	Ca2–O19	2.5981(10)
Ca1–O7	2.6293(11)		
O3–Ca1–O5	80.62(3)	N1–Ca1–O7	137.98(4)
O3–Ca1–O1	126.66(3)	N2–Ca1–O7	62.26(3)
O5–Ca1–O1	90.07(4)	O9–Ca1–O7	69.34(4)
O3–Ca1–N3	75.45(4)	O11–Ca1–O7	90.01(4)
O5–Ca1–N3	136.78(4)	O22–Ca2–O21	80.26(5)
O1–Ca1–N3	133.01(4)	O22–Ca2–O17	156.88(5)
O3–Ca1–N1	63.63(4)	O21–Ca2–O17	89.34(5)
O5–Ca1–N1	79.17(4)	O22–Ca2–O15	106.83(5)
O1–Ca1–N1	63.04(4)	O21–Ca2–O15	155.37(4)
N3–Ca1–N1	119.25(4)	O17–Ca2–O15	91.21(4)
O3–Ca1–N2	140.28(4)	O22–Ca2–O13	78.68(5)
O5–Ca1–N2	62.83(3)	O21–Ca2–O13	79.19(4)
O1–Ca1–N2	71.28(4)	O17–Ca2–O13	79.11(4)
N3–Ca1–N2	120.83(4)	O15–Ca2–O13	125.05(4)
N1–Ca1–N2	119.41(4)	O22–Ca2–N4	82.02(5)
O3–Ca1–O9	97.19(4)	O21–Ca2–N4	140.78(4)
O5–Ca1–O9	156.57(4)	O17–Ca2–N4	93.63(4)
O1–Ca1–O9	72.41(3)	O15–Ca2–N4	63.74(4)
N3–Ca1–O9	63.22(3)	O13–Ca2–N4	63.13(3)
N1–Ca1–O9	79.02(4)	O22–Ca2–N5	131.33(4)
N2–Ca1–O9	122.52(4)	O21–Ca2–N5	77.89(4)
O3–Ca1–O11	72.09(4)	O17–Ca2–N5	64.96(3)
O5–Ca1–O11	75.33(3)	O15–Ca2–N5	80.06(4)
O1–Ca1–O11	154.60(4)	O13–Ca2–N5	137.16(4)
N3–Ca1–O11	63.32(3)	N4–Ca2–N5	137.84(4)
N1–Ca1–O11	131.64(4)	O22–Ca2–O19	72.20(4)
N2–Ca1–O11	83.50(4)	O21–Ca2–O19	81.81(4)
O9–Ca1–O11	126.46(3)	O17–Ca2–O19	126.94(3)
O3–Ca1–O7	145.22(4)	O15–Ca2–O19	78.23(4)
O5–Ca1–O7	124.31(3)	O13–Ca2–O19	147.45(4)
O1–Ca1–O7	81.09(4)	N4–Ca2–O19	124.91(4)
N3–Ca1–O7	69.85(4)	N5–Ca2–O19	62.02(3)
<i>Compound 2</i>			
Zr1–O1	2.2276(9)	Zr1–O3	2.2270(8)
Zr1–N1	2.3526(9)	Zr1–O5	2.2171(8)
Zr1–N2	2.3489(13)		
O5–Zr1–O5 ⁱ ₁	134.78(5)	O1–Zr1–N2	136.64(2)
O3–Zr1–N2	70.67(2)	O5–Zr1–N1	69.84(3)
O5–Zr1–O3	89.14(3)	N1–Zr1–N1 ⁱ ₁	121.96(5)
O5 ⁱ ₁ –Zr1–O3	76.14(3)	O3 ⁱ ₁ –Zr1–N1	134.98(3)
O3 ⁱ ₁ –Zr1–O3	141.34(5)	O3–Zr1–N1	67.32(3)
O5–Zr1–O1 ⁱ ₁	141.32(3)	O1 ⁱ ₁ –Zr1–N1	71.51(3)
O3–Zr1–O1 ⁱ ₁	77.37(3)	O1–Zr1–N1	67.15(3)
O5–Zr1–O1	77.20(3)	N2–Zr1–N1	119.02(2)
O5 ⁱ ₁ –Zr1–O1	141.32(3)	O5–Zr1–N1 ⁱ ₁	135.86(3)
O3–Zr1–O1	134.43(3)	O5 ⁱ ₁ –Zr1–N1 ⁱ ₁	69.84(3)
O1 ⁱ ₁ –Zr1–O1	86.72(5)	O3 ⁱ ₁ –Zr1–N1 ⁱ ₁	67.32(3)
O5–Zr1–N2	67.39(2)	O3–Zr1–N1 ⁱ ₁	134.98(3)
N2–Zr1–N1 ⁱ ₁	119.02(2)		

(Continued)

Table 2. (Continued).

Symmetry codes: (i) $-x + 2, y, -z + 1/2$			
<i>Compound 3</i>			
Cd1–N1	2.227(2)	Cd1–O1	2.3397(19)
N1 ⁱ –Cd1–N1	180.0	O1–Cd1–O1 ⁱⁱ	96.25(3)
N1–Cd1–O1	70.74(4)	N1–Cd1–O1 ⁱⁱⁱ	70.74(4)
N1–Cd1–O1 ⁱⁱ	109.26(4)	O1–Cd1–O1 ⁱⁱⁱ	141.48(9)
Symmetry codes: (i) $y - 1/4, -x + 1/4, -z + 1/4$; (ii) $-y + 1/4, x + 1/4, -z + 1/4$; (iii) $-x, -y + 1/2, z$			
<i>Compound 4</i>			
Hg1–N1	2.190(4)	Hg1–O1	2.442(3)
N1 ⁱ –Hg1–N1	180.0	O1 ⁱⁱ –Hg1–O1 ⁱ	142.30(13)
N1 ⁱ –Hg1–O1 ⁱⁱ	71.15(6)	O1 ⁱⁱⁱ –Hg1–O1 ⁱ	95.99(4)
N1–Hg1–O1 ⁱⁱ	108.85(6)	N1 ⁱ –Hg1–O1	108.85(6)
N1 ⁱ –Hg1–O1 ⁱⁱⁱ	108.85(6)	N1–Hg1–O1	71.15(6)
N1–Hg1–O1 ⁱⁱⁱ	71.15(6)	O1 ⁱⁱ –Hg1–O1	95.99(4)
O1 ⁱⁱ –Hg1–O1 ⁱⁱⁱ	95.99(4)	O1 ⁱⁱⁱ –Hg1–O1	142.30(13)
N1 ⁱ –Hg1–O1 ⁱ	71.15(6)	O1 ⁱ –Hg1–O1	95.99(4)
Symmetry codes: (i) $y - 1/4, -x + 5/4, -z + 1/4$; (ii) $-y + 5/4, x + 1/4, -z + 1/4$; (iii) $-x + 1, -y + 3/2, z$			

N1–Ca1–N2 equals 359.5(4)° and indicates the Ca1 is located in the center of the N1N2N3 plane. Any three oxygens form a triangle around Ca(II). The angles between oxygens demonstrate that they are approximately eclipsed, so a prism with three caps of three nitrogens on its faces is proposed. Consequently, the coordination polyhedron around Ca(II) is a distorted tricapped trigonal prism. In [Ca(pydcH₂)(pydc)(H₂O)₂] in **1**, Ca(II) is eight coordinate by four carboxylate oxygens and two nitrogens from (pydc)²⁻ and neutral pydcH₂ ligands as well as O21 and O22 from water molecules, giving a distorted dodecahedron. As shown in figure 2, the carboxyl groups of pydcH₂, pydcH⁻, and (pydc)²⁻ ligands and water molecules are involved in intermolecular O–H···O hydrogen bonding and form various hydrogen bond networks. This intermolecular interaction connected the various components into a 3D network.

Some complexes of imidazole and 2-methylimidazole with pyridine-2,6-dicarboxylic acid and metal salts have been published previously [20, 21], bis(2-methylimidazolium 2,6-dicarboxypyridine) M(II) salts [M = Zn, Cu, Ni, Co, Mn] and bis(imidazolium 2,6-pyridinedicarboxylate) M(II) trihydrate complexes, where M = Mn²⁺, Co²⁺, Ni²⁺, Cu²⁺, or Zn²⁺. In all of those complexes, imidazole fragments are counter cations and balanced the charge of anionic complexes; the coordination spheres around metal centers exhibit octahedral geometry *via* two pyridine-2,6-dicarboxylate ligands [20, 21]. The cations and anions in those complexes were tightly connected *via* hydrogen bond interactions. Our complexes are in agreement with those complexes previously reported [20, 21].

The crystallographic data of **2** are given in table 1, selected bond lengths and angles and selected intermolecular hydrogen bonds parameters are listed in tables 2 and 3, respectively. As illustrated in figure 3, **2** consists of a nine-coordinate anionic complex and two cationic fragments. In the anionic complex, three (pydc)²⁻ ligands are coordinated to Zr(IV) in a tridentate chelating fashion through three pyridine nitrogens and six oxygens of carboxylate groups. All Zr–O distances are nearly equal to each other and the Zr–N bonds are similar (table 2). The sum of bond angles N1–Zr1–N1', N2–Zr1–N1', and N2–Zr1–N1 is 360°,

Table 3. Hydrogen bond geometry of **1–4**.

D–H···A	D–H	H···A	D···A	D–H···A
<i>Compound 1</i>				
O1S–H1SA···O10	0.85	2.02	2.863(2)	174
O2–H2···O15	0.96(3)	1.58(3)	2.519(2)	164(2)
O2–H2···O16	0.96(3)	2.56(2)	3.319(2)	136(2)
O1S–H1SB···O4 ⁱ	0.85	1.92	2.741(2)	163
O3S–H3SB···O10	0.85	1.15	2.924(2)	151
O4S–H4SA···O6 ⁱⁱ	0.85	2.03	2.878(3)	176
O4S–H4SB···O16 ⁱⁱⁱ	0.85	2.18	2.864(3)	138
N6–H6···O4 ^{iv}	0.84(4)	1.86(4)	2.689(2)	168(3)
N7–H7···O11 ^v	0.87(2)	2.45(3)	3.149(2)	137(3)
O8–H8···O14 ^{vi}	0.76(3)	1.85(3)	2.605(2)	173(3)
O12–H12A···O13 ^{vii}	0.85(2)	1.70(3)	2.533(2)	166(2)
O18–H18A···O5 ^{iv}	0.99(3)	1.53(3)	2.500(2)	166(2)
O19–H19A···O9	0.91(3)	1.68(3)	2.582(2)	170(2)
O21–H21A···O3S	0.87	1.96	2.826(2)	173
O22–H22A···O14 ^{vi}	0.86(3)	1.90(3)	2.765(2)	174(3)
O22–H22B···O10	0.89(3)	1.92(3)	2.810(2)	177(2)
C10–H10···O2S ^{viii}	0.93	2.52	3.398(2)	157
Symmetry codes: (i) $1-x, 1-y, -z$; (ii) $1-x, -y, -z$; (iii) $-1+x, y, z$; (iv) $x, 1+y, z$; (v) $-1+x, 1+y, z$; (vi) $2-x, 1-y, 1-z$; (vii) $x, -1+y, z$; (viii) $1+x, -1+y, z$				
<i>Compound 2</i>				
N4–H···O6	0.84(3)	2.28(3)	2.915(2)	132(2)
N4–H···O2 ⁱ	0.84(3)	2.45(2)	3.037(2)	128(3)
C12–H12···O4 ⁱⁱ	0.93	2.16	3.079(2)	169
C15–H15A···O6 ⁱⁱⁱ	0.96	2.52	3.394(3)	151
Symmetry codes: (i) $-x+3/2, 1/2-y, -z$; (ii) $2-x, -y, 1-z$; (iii) $3/2-x, 1/2+y, 1/2-z$				
<i>Compound 3</i>				
N2–H···O1S	0.83(3)	1.89(4)	2.727(5)	178(5)
O1S–H1S···O2S ⁱ	0.83(3)	2.03(3)	2.814(6)	157(3)
O1S–H2S···O1	0.85(4)	1.88(4)	2.729(4)	175(6)
C6–H6···O ⁱⁱ	0.93	2.54	3.421(5)	159
Symmetry codes: (i) $5/4-x, -1/4+y, 1/4+z$; (ii) $3/4-x, -1/4+y, -1/4+z$				
<i>Compound 4</i>				
N2–H2···O3 ⁱ	0.78	1.96(6)	2.727(7)	169(6)
O3–H3A···O4A ⁱⁱ	0.94(3)	1.76(3)	2.694(8)	173(4)
O3–H3B···O1 ⁱⁱⁱ	0.94(2)	1.82(5)	2.715(5)	158(7)
C5–H5···O2 ^{iv}	0.93	2.49	3.373(7)	158
Symmetry codes: (i) $-1+x, y, z$; (ii) $-3/4+x, 5/4-y, 1/4-z$; (iii) $1-x, 3/2-y, z$; (iv) $3/4-x, -5/4+y, -1/4+z$				

indicating Zr1 is located in the center of the N1N1'N2 plane. Any three oxygens form a triangle around Zr(IV). The angles between oxygens demonstrate that they are eclipsed, so a prism with three caps of three nitrogens on its faces is proposed. Therefore, the coordination polyhedron around Zr(IV) is a distorted tricapped trigonal prism. The crystal structure of **2** is comparable with similar Zr(IV) compounds, (pydaH)₂[Zr(pydc)₃]·5H₂O [22] and (pipzH₂)[Zr(pydc)₃]·8H₂O [20], in which pyda is pyridine-2,6-diamine and pipz is piperazine. The average values of Zr–O and Zr–N bond lengths are also in agreement with previous reports of Zr(IV) complexes with pyridine-2,6-dicarboxylate [22, 23]. Although three compounds have a nine-coordinate anionic fragment with similar bond lengths and angles around Zr(IV), **2** has a less distorted coordination. Another aspect of the crystal structure of **2** is the presence

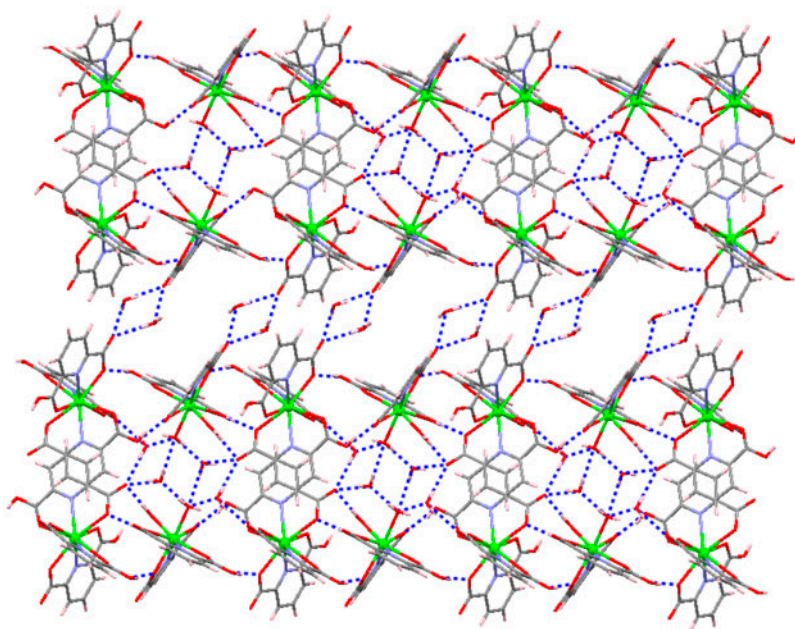


Figure 2. A section of the robust O–H···O hydrogen bond network and water clusters that link the layers of **1** [the dashed blue lines show donor–acceptor distances of hydrogen bonds] (see <http://dx.doi.org/10.1080/00958972.2015.1079627> for color version).

of C–H··· π stacking interactions. The H··· π distances are 2.75 Å. In **2**, a portion of hydrogen bonding motif between anions and cations formed a 1D zigzag chain. The anionic complexes connected head-to-tail to cationic fragments by N–H···O hydrogen bonds between H–N4 bonded to O2 and O6 of the anions. The O2–H and O6–H distances are 2.45(2) and 2.28(3) Å, respectively. The intermolecular hydrogen bonds and C–H··· π stacking interactions play important roles in formation of the 3D supramolecular network of **2**.

Compounds **3** and **4** display isostructural features and crystallize in a tetragonal space group. The crystallographic data and detailed information on the structure solution and refinement for **3** and **4** are given in table 1. Selected bond distances and angles are listed in table 2, and selected intermolecular hydrogen bond parameters are listed in table 3. The asymmetric unit of **3** and **4** consists of one $[M(\text{pydc})_2]^{2-}$ anion, two 2-methylimidazolium cations, and eight co-crystallization water molecules. The presence of 2-methylimidazolium facilitated the proton-transfer process supporting the formation of the Cd(II) and Hg(II) complexes. The Cd^{II} and Hg(II) ions in **3** and **4** are six coordinate by two tridentate pydc^{2-} anions, and the geometry of the resulting MN_2O_4 coordination can be described as a distorted octahedron. In many cases reported, pyridine-2,6-dicarboxylate as a chelating ligand connects metal centers in a tridentate fashion. Consequently, many different coordination geometries were obtained with coordination of this ligand to metal ions. Six and nine coordination geometries of Cd(II) with $(\text{pydc})^{2-}$ ligands have been reported previously [10(b)]. The nine-coordinate Cd(II) complexes with $(\text{pydc})^{2-}$ ligands show distorted tricapped trigonal prisms [10b], while the six-coordinate Cd(II) complexes demonstrated distorted octahedral geometry.

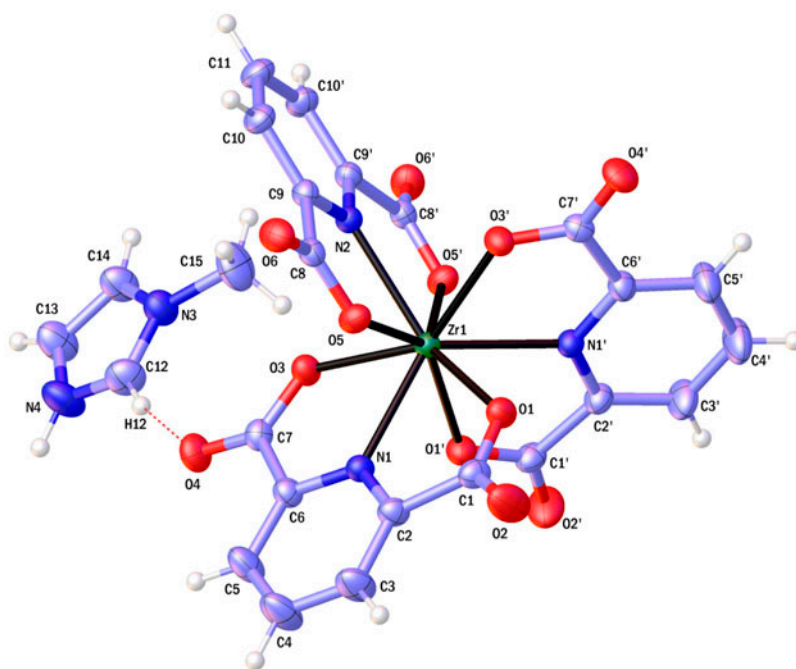


Figure 3. ORTEP diagram of $(1\text{-mimH})_2[\text{Zr}(\text{pydc})_3]$ (**2**). Non H-atoms represented as displacement ellipsoids are plotted at 50% probability level, while hydrogens are shown as small spheres of arbitrary radius.

The bond angles around Cd(II) ion, involving *trans* pairs of donors, are in the range of $141.48(9)^\circ$ – 180° , and for the *cis* pairs of donors, this range is $70.74(4)^\circ$ – $109.26(4)^\circ$ (table 2). These values indicate a large distortion from ideal octahedral geometry due to binding of dipicolinate ligands to Cd(II) in an *O,N,O'*-tridentate fashion in the anionic complex. The dihedral angle between two coordinated $(\text{pydc})^{2-}$ groups is 90° ; therefore, the ligands are perpendicular to each other (figure 4). In **3**, the Cd(II) complexes and co-crystallized water molecules are linked by $\text{O}-\text{H}\cdots\text{O}$ hydrogen bonds and formed 2D sheets. 2-Methylimidazolium fragments trap in the cavities of anionic complexes and water molecules. Besides the cations connected to anionic complexes, water molecules *via* $\text{N}-\text{H}\cdots\text{O}$ hydrogen bonds and constructed 2D networks (figure 5). In **3**, one of the water molecules (O2S) is disordered. Another aspect in this crystal structure is the existence of water clusters. Water clusters are generated by hydrogen bonds between water molecules. The water clusters in **3** consist of dimeric and tetrameric water chains made by O1S and O2S. Molecular structure of **4** is illustrated in figure 6. The bond distances (Hg–N and Hg–O) and coordination geometry around Hg(II) in **4** are in agreement with those reported previously [24, 25].

The patterns of hydrogen bonds in **4** are similar to **3**. Cooperation of $\text{O}-\text{H}\cdots\text{O}$ hydrogen bonds made infinite various membered chain and rings in these crystal structures (figure 5). Also the $\text{O}-\text{H}\cdots\text{O}$ hydrogen bonds formed infinite one and 2-D chains in many directions. The hydrogen bonds connect the co-crystallized water molecules to neighboring complexes with $\text{O}\cdots\text{O}$ distances of 2.694(8) and 2.715(5) Å in **4**. Intermolecular $\text{O}-\text{H}\cdots\text{O}$ and $\text{N}-\text{H}\cdots\text{O}$ interactions formed various types of hydrogen bond networks. These intermolecular interactions connected the various components into a 3D network in **3** and **4**. As seen in figure 7, cationic fragments have been trapped between anionic complexes and water molecules as

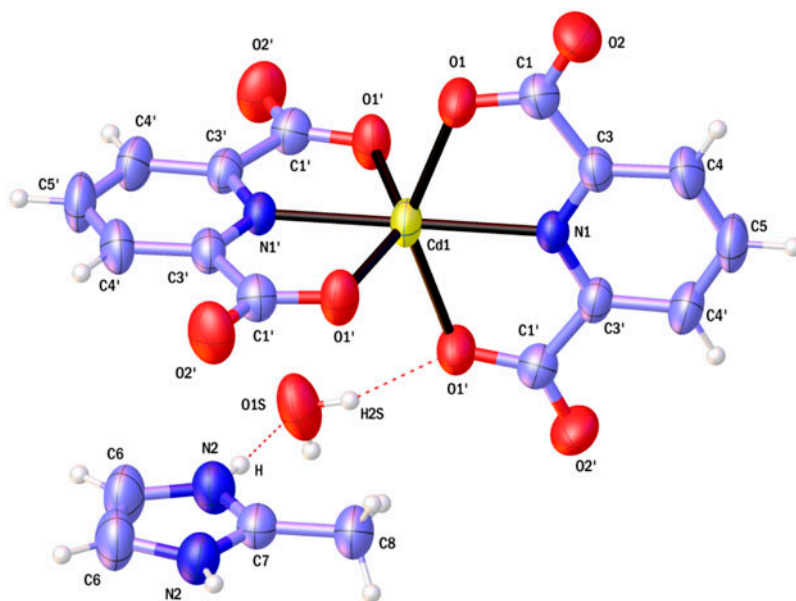


Figure 4. ORTEP diagram of $(2\text{-mimH})_2[\text{Cd}(\text{pydc})_2]\cdot 8\text{H}_2\text{O}$ (**3**). Non H-atoms represented as displacement ellipsoids are plotted at 50% probability level, while hydrogens are shown as small spheres of arbitrary radius. Disordered water has been omitted for clarity.

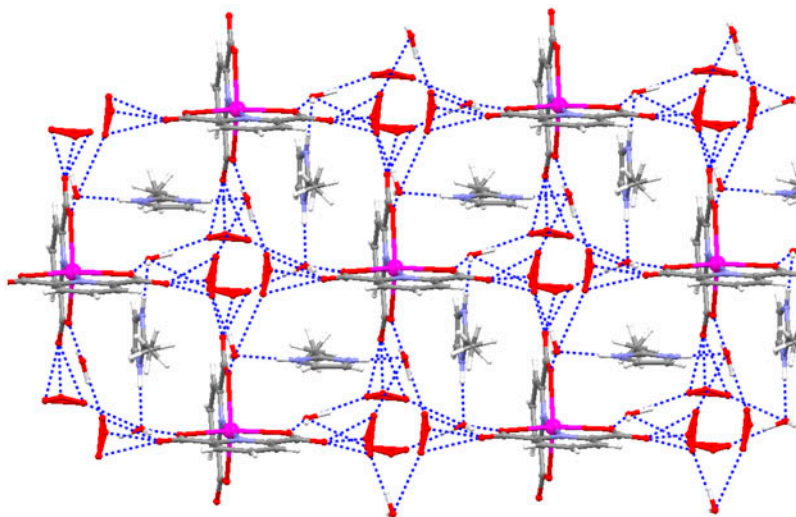


Figure 5. The extended 2D network of **3** interconnected by hydrogen bonds between water molecules, cations, and anionic complexes. Water clusters connect anionic complexes.

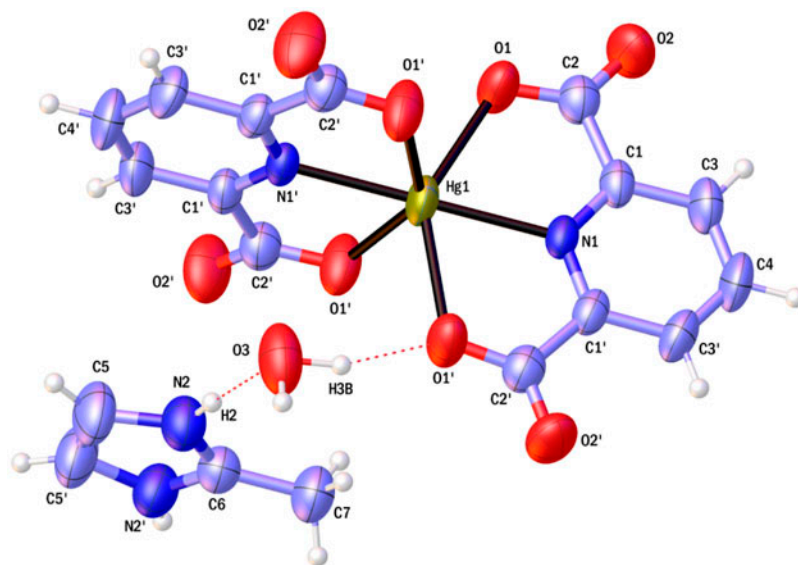


Figure 6. ORTEP diagram of $(1\text{-mimH})_2[\text{Hg}(\text{pydc})_2]\cdot 8\text{H}_2\text{O}$ (**4**). Non H-atoms represented as displacement ellipsoids are plotted at 50% probability level, while hydrogens are shown as small spheres of arbitrary radius. Disordered water has been omitted for clarity.

was true for **3**. Also hydrogen bonding interactions between water molecules result in four-membered water rings. The tetramers are formed by O3 and O4B with O4B disordered. In the crystal structures of **3** and **4**, C–H $\cdots\pi$ stacking interactions connect anionic complexes and formed 1D polymeric chains [figure 8(a)]. The strong and weak hydrogen bond interactions (O–H \cdots O, N–H \cdots O and C–H \cdots O) formed a porous network in **3** and **4** [figure 8(b)]; these intermolecular interactions accompanied with C–H $\cdots\pi$ stacking interactions play important roles in the formation of 3D supramolecular networks of **3** and **4**. The range of hydrogen bond interactions in **4** is slightly smaller than **3**; consequently, some of the cell parameters and cell volume in this compound is slightly smaller.

3.3. Thermal analysis

The TG–DTG and DTA curves of **1** show an endothermic peak from room temperature to 280 °C that corresponds to loss of five water molecules. Then, the complex decomposed, accompanied by the loss of organic ligands. The final decomposition product was CaO. The first endothermic peak of **2** between 30 and 400 °C corresponds to loss of 2-methylimidazolium cations. In the following stage between 400 and 700 °C, the complex began to decompose and released organic ligands. The TG curve for **3** illustrates this compound is stable from room temperature to 180 °C. From 180 to 250 °C, the co-crystallized water molecules were removed. The TGA curve for **4** demonstrates the first weight loss from 35 to 201 °C from loss of uncoordinated water. The second stage, an endothermic peak between 201 and 279 °C, corresponds to loss of two $(1\text{-mimH})^+$ cations (found 38.4, Calcd 39.6%). Then, the complex began to decompose upon further heating from 280 to 564 °C accompanied by loss of pydc. The main product was HgO with residual value of 23.094%; theoretical residual value was 25.9%. All TG curves are given in figures 7S–10S.

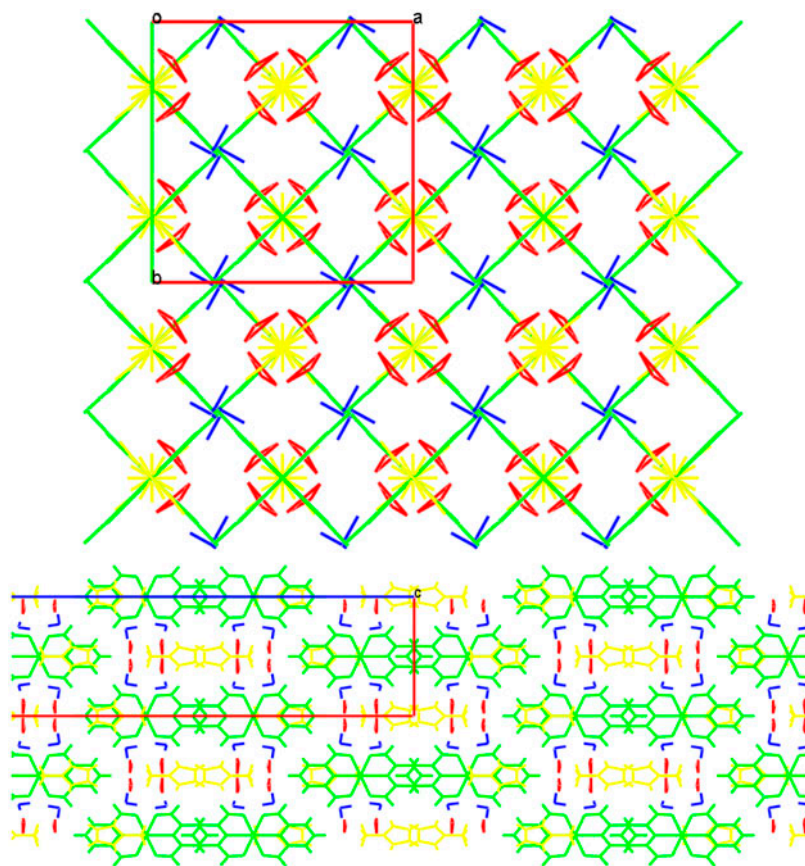


Figure 7. A view of trapping cationic fragments between anionic complexes and water molecules in a (top) and b directions (bottom).

3.4. Solution studies

In preliminary experiments, the fully protonated forms of pydc (L), 2-mim (Q), and 1-mim (Q') were titrated with a standard NaOH solution to obtain some information about their protonation constants as the building blocks of the pydc/2-mim and pydc/1-mim proton-transfer systems. The protonation constants of pydc, 2-mim, and 1-mim were calculated by fitting the pH-volume data (figures 11Sa, 12Sa, 12Sb, and 13Sa) to the Hyperquad 2008 program. The results are summarized in table 4. The resulting $\log\beta$ values are in satisfactory agreement with those reported for 2-mim and 1-mim in the literature [26, 27], but in this study, two protonation constants were found for each of them. The evaluation of the equilibrium constants for the reactions of pydc with 2-mim or 1-mim in different protonation forms was accomplished through comparison of the calculated and experimental pH profiles, obtained with both pydc and 2-mim or 1-mim present [28, 29]. The results are shown in table 4. Distribution diagrams for 2-mim are shown in figure 9(a) and (b). The most abundant proton-transfer species present for pydc/2-mim system at pH 7.0 (85.92%), 3.7 (80.4%), and 2.0 (62.56%) are [2-mimHpydc] ($\log K = 4.34$), [2-mimHpydcH] ($\log K = 4.40$) and {[2-mimHpydcH₂] ($\log K = 4.64$), [2-mimH₂pydcH] ($\log K = 5.33$)}. For

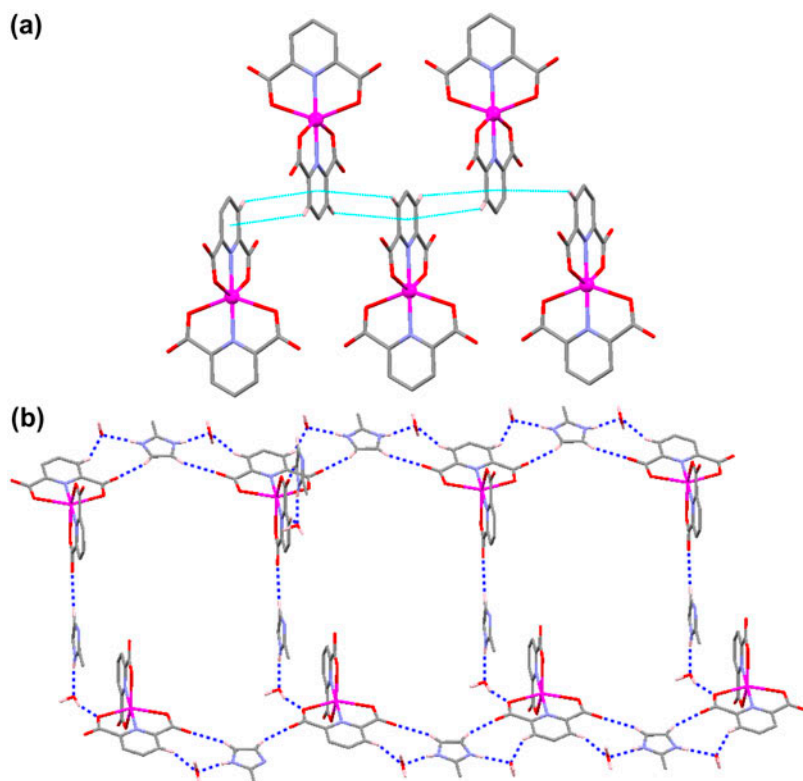


Figure 8. (a) C–H $\cdots\pi$ interaction in **4**, (b) porosity network of **4** made by strong and weak hydrogen bonds. Some of the hydrogens were omitted for clarity.

Table 4. Overall and stepwise protonation constants of pydc/2-mim and 1-mim and recognition constants for pydc/2-mim and pydc/1-mim in aqueous solution at 25 ± 0.1 °C and $\mu = 0.1$ M NaNO₃ or NaClO₄.

Stoichiometry				Log β	Equilibrium quotient K	Log K	Max (%)	At pH
1-mim	2-mim	pydc	h					
0	0	1	1	4.95		4.95	92.6	3.5
0	0	1	2	7.10		2.146	58.28	2.0
0	1	0	1	7.95		7.95	99.80	3.5–5.9
0	1	0	2	9.40		1.45	22.27	2.0
1	0	0	1	7.21		7.21	99.81	3.4–4.7
1	0	0	2	8.26		1.05	10.08	2.0
0	1	1	1	12.29	[2-mimHpydc]/[pydc][2-mimH]	4.34	85.92	7.0–7.1
0	1	1	2	17.30	[2-mimHpydcH]/[pydcH][2-mimH]	4.40	80.4	3.7
0	1	1	3	19.68	[2-mimHpydcH ₂]/[pydcH ₂][2-mimH]	4.64	62.5	2.0
					[2-mimH ₂ pydcH]/[pydcH][2-mimH ₂]	5.33		
1	0	1	1	11.29	[1-mimpydcH]/[1-mimH][pydc]	4.08	90.9	6.7
1	0	1	2	16.47	[1-mimHpydcH]/[pydcH][1-mimH]	3.85	69.2	3.6
1	0	1	3	19.05	[1-mimHpydcH ₂]/[pydcH ₂][1-mimH]	3.64	64.8	2.0
					[1-mimH ₂ pydcH]/[pydcH][1-mimH ₂]	5.84		

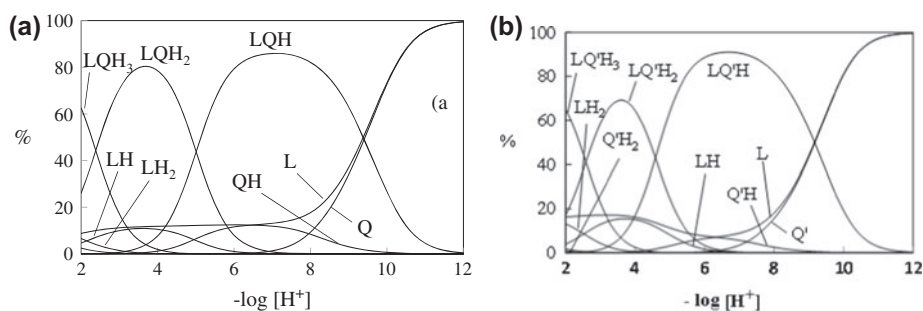


Figure 9. Distribution diagrams of proton-transfer interaction of 2-mim (Q) (a) or 1-mim (Q') (b) with pydc (L).

the pydc/1-mim system at pH 6.7 (90.9%), 3.6 (69.2%), 2.0 (64.8%) are [1-mimpydcH] ($\log K = 4.08$), [1-mimpydcH₂] ($\log K = 3.85$) and {[1-mimH₂pydcH]} ($\log K = 5.84$).

In order to evaluate the stoichiometry and stability of Hg²⁺, Ca²⁺, Cd²⁺, and Zr⁴⁺ complexes with pydc/2-mim or pydc/1-mim proton-transfer systems in aqueous solution, the equilibrium potentiometric pH titration profiles of pydc, 2-mim, 1-mim and their 1 : 1 mixtures were obtained in the absence and presence of the Hg²⁺, Ca²⁺, Cd²⁺, and Zr⁴⁺ ions. The resulting pH profiles are shown in figures 11Sa, 12Sa, 12Sb, 13Sa, 10a, 10c, and 11a.

Table 5. Overall stability constants of 2-mim or 1-mim/pydc/Mⁿ⁺ (q or $q'/l/m$) binary and ternary systems in aqueous solution at 25 ± 0.1 °C and $\mu = 0.1$ M NaNO₃ or NaClO₄.

System	m	l	q	q'	h	Log β	Max (%)	At pH
Hg ²⁺ /pydc	1	1	0	0	0	7.11	25.32	>6
	1	2	0	0	0	11.078	74.66	>7.6
	1	2	0	0	1	15.556	98	2
Cd ²⁺ /2-mim	1	0	1	0	0	3.27	54.49	8.3–10.6
	1	0	2	0	0	5.78	22.05	9.2–10.8
	1	0	1	0	2	-19.41	91.92	12.0
Ca ²⁺ /2-mim	1	0	1	0	1	10.81	44.84	2.5–6.4
	1	0	2	0	1	13.93	23.14	8.40
	1	0	2	0	2	17.03	Negligible	—
Hg ²⁺ /2-mim	1	2	0	0	0	17.124	75.08	6
	1	2	0	0	1	22.194	99.92	2
	1	1	0	0	-1	6.75	93.76	8.9
Zr ⁴⁺ /1-mim	1	1	0	0	-2	-3.651	97.52	12
	1	0	0	1	0	6.75	91.76	4.3
	1	0	0	3	0	16.28	96.32	2.3–5/9
Cd ²⁺ -pydc/2-mim	1	0	0	1	-1	-3.58	9.97	12.0
	1	0	0	1	-2	-16.02	2.62	12.0
	1	2	1	0	1	22.99	59.63	7.6
Ca ²⁺ -pydc/2-mim	1	2	1	0	2	29.06	83.52	4.1
	1	2	1	0	1	21.49	43.28	5.9–7.7
	1	1	1	0	1	17.04	51.49	4.7
Hg ²⁺ -pydc/2-mim	1	1	1	0	0	9.10	93.92	>11.8
	1	1	2	0	0	24.773	89.36	9.8
	1	1	1	0	1	27.599	9.80	2–4.2
Zr ⁴⁺ -pydc/1-mim	1	2	1	0	1	32.467	90.08	2–4.0
	1	3	0	1	1	33.54	96.16	6.2–9.4
	1	3	0	1	2	37.50	1.84	5.4
	1	3	0	1	3	44.30	96.4	3.9–4.6

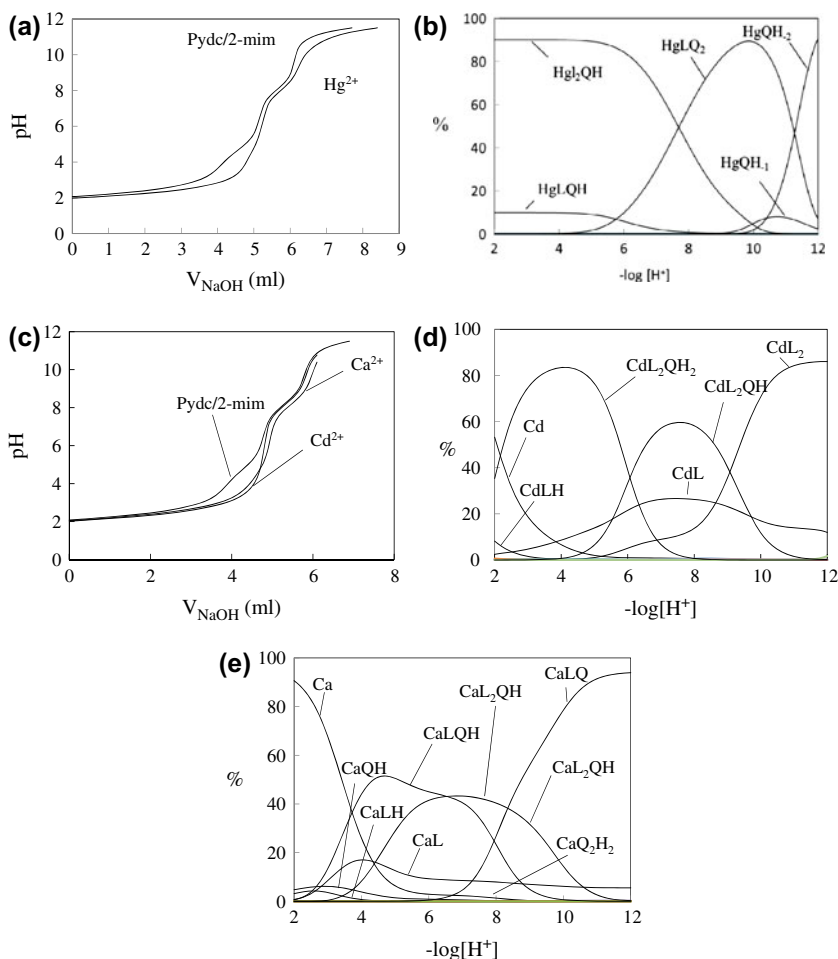


Figure 10. Potentiometric titration curves of pydc/2-mim in the absence and presence of Hg^{2+} (a), Cd^{2+} and Ca^{2+} ions (c) with 0.10016 M NaOH in aqueous solution at 25 ± 0.1 °C and $\mu = 0.1$ M NaNO_3 or NaClO_4 , and the corresponding distribution diagrams (b, d, and e).

The titration in the presence of metal ions was stopped when precipitate was observed. The 2-mim forms relative weak complexes with Ca^{2+} and Cd^{2+} similar to what was seen for other M^{2+} cations [26, 27], while the complexation between 1-mim and Zr^{4+} ion is relatively strong. The interaction for 2-mim/ Hg^{2+} is similar to imidazole/ Hg^{2+} [30] and pydc- M^{n+} systems [12, 24, 31–34] and is relatively strong, except for the pydc- Ca^{2+} system. The cumulative stability constants of $\text{M}_m\text{L}_l\text{Q}_q\text{H}_h$, β_{mlqh} , are defined in our previous publications [13, 26] where M, L, Q, Q', and H are metal ion, pydc, 2-mim, 1-mim, and proton, respectively, and m , l , q , and h are the respective stoichiometric coefficients.

The cumulative stability constants were evaluated by fitting the corresponding pH-volume data to the Hyperquad 2008 program and the resulting values for the most likely complexed species in aqueous solutions are also included in table 5. The corresponding distribution diagrams are shown in figures 11Sb, 12Sc, 12Sd, 12Se, 13Sb, 10(b), (d), (e), and 11(b).

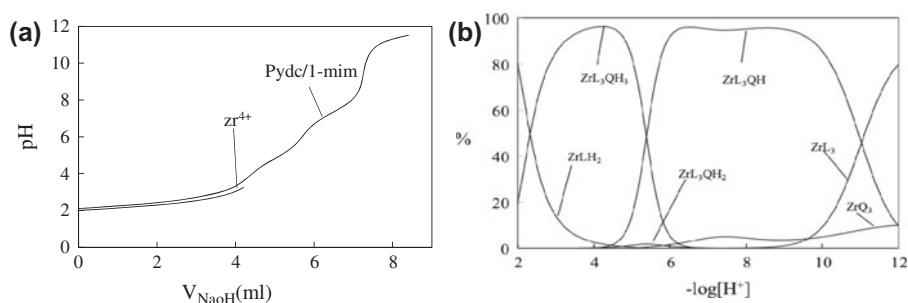


Figure 11. Potentiometric titration curves of pydc/1-mim in the absence and presence of Zr^{4+} ions with 0.10016 M NaOH in aqueous solution at 25 ± 0.1 °C and $\mu = 0.1$ M $NaNO_3$, (a) and the corresponding distribution diagram (b).

Confirming previous results [29–33], the cited distribution diagrams and table 5 in the case of pydc(L), as ligand, show that the most likely species for Ca^{2+} are CaL , $CaLH$, CaL_2 , CaL_2H , and CaL_2H_2 ; for Cd^{2+} are CdL , $CdLH$, CdL_2 , and CdL_2H_2 ; for Zr^{4+} are ZrL_3 , $ZrLH$, $ZrLH_2$, ZrL_2 , ZrL_2H , ZrL_3 , ZrL_3H , and ZrL_3H_2 . Figure 11Sb and table 5 show the species for Hg^{2+} -pydc binary system are HgL_2 , HgL_2H , $HgLH_{1,1}$, and $HgLH_{1,2}$.

Figures 12Sc–e and table 5 show for 2-mim/ M^{2+} system, the most likely species for Hg^{2+} are HgQ_2 , HgQ_2H , $HgQH_{1,1}$, and $HgQH_{1,2}$; for Ca^{2+} are CaQ , CaQ_2 , and $CaQH_2$ and for Cd^{2+} are $CdQH$, CdQ_2H , and CdQ_2H_2 .

Figure 13Sb and table 5 show for 1-mim/ Zr^{4+} system, the most likely species are ZrQ' , ZrQ'_3 , $ZrQ'H_{1,1}$, and $ZrQ'H_{1,2}$.

Figures 11(d), (e), and (b) and table 5 reveal the formation of a variety of ternary complexes between the above-mentioned cations and the proton-transfer system at different ranges of pH. The predominant species for Cd^{2+} are CdL_2QH (at pH 7.6) and CdL_2QH_2 (at pH 4.1); for Ca^{2+} CaL_2QH (at pH 5.9–7.7), $CaLQH$ (at pH 4.7) and $CaLQ$ (at pH > 11.8); for Hg^{2+} are $HgLQ_2$ (at pH 9.8), $HgLQH$ (at pH 2.0–4.2), and HgL_2QH (at pH 2.0–4.0); and for Zr^{4+} are $ZrL_3Q'H$ (at pH 6.2–9.4), $ZrL_3Q'H_2$ (at pH 5.4), and $ZrL_3Q'H_3$ (at pH 3.9–4.6). The stoichiometry of CdL_2QH , CaL_2QH , HgL_2QH , and $ZrL_3Q'H_2$ ternary complexes existing in aqueous solution is the same or similar to that reported for the corresponding isolated complexes in the solid state.

4. Conclusion

Four new supramolecular compounds, $(2\text{-mimH})[Ca(\text{pydcH})_3][Ca(\text{pydcH}_2)(\text{pydc})(\text{H}_2\text{O})_2]\cdot 4\text{H}_2\text{O}$ (**1**), $(1\text{-mimH})_2[Zr(\text{pydc})_3]$ (**2**), $(2\text{-mimH})_2[Cd(\text{pydc})_2]\cdot 8\text{H}_2\text{O}$ (**3**), and $(2\text{-mimH})_2[Hg(\text{pydc})_2]\cdot 8\text{H}_2\text{O}$ (**4**), with dipicolinic acid and methylimidazole have been synthesized and characterized. To investigate the coordination abilities of ligands, we have used transition metal nitrate or chloride salts, yielding four mononuclear coordination compounds. For all compounds, the dicarboxylic ligands are deprotonated and methylimidazole is protonated and balances the charge. The $(\text{pydc})^{2-}$ ligands are coordinated tridentate to the metal center. Compound **1** is an interesting example of a compound containing anionic

and neutral metal complexes with different coordination geometries. The crystal packing of **1–4** show 3D networks formed through H-bonds involving water, NH groups of cations, carboxylate anions, and $\pi\cdots\pi$ stacking interactions. The stoichiometry and stability constants of the proton-transfer systems and their metal ion complexes obtained from solution studies are in agreement with the structural results.

Supplementary material

CCDC-935783, 935784, 935786, and 935787 contain the supplementary crystallographic data for **1–4**, respectively. These data can be obtained free of charge at <http://www.ccdc.cam.ac.uk/conts/retrieving.html>, or from the Cambridge Crystallographic Data Center, 12 Union Road, Cambridge CB2 1EZ, UK (Fax: 0044 1223 336 033; E-mail: deposit@ccdc.cam.ac.uk).

Disclosure statement

No potential conflict of interest was reported by the authors.

Supplemental data

Supplemental data for this article can be accessed here [\[http://dx.doi.org/10.1080/00958972.2015.1079627\]](http://dx.doi.org/10.1080/00958972.2015.1079627).

References

- [1] M.B. Gholivand, A. Azadbakht, A. Pashabadi. *Electroanalysis*, **23**, 364 (2011).
- [2] Z. Derikvand, M.M. Olmstead. *Acta Crystallogr., Sect. E: Struct. Rep. Online*, **66**, m642 (2010).
- [3] L. Yang, S. Song, H. Zhang, W. Zhang, L. Wu, Z. Bu, T. Ren. *Synth. Met.*, **162**, 261 (2012).
- [4] E. Norkus, I. Stalnioniene. *Chemija (Vilnius)*, **13**, 194 (2002).
- [5] A.T. Çolak, F. Çolak, O.Z. Yeşilel, E. Şahin. *J. Iran. Chem. Soc.*, **7**, 384 (2010).
- [6] O.Z. Yeşilel, İnci İlker, M.S. Refat, H. Ishida. *Polyhedron*, **29**, 2345 (2010).
- [7] Q. Shuai, S. Chen, H. Geng, S. Gao. *Inorg. Chim. Acta*, **379**, 145 (2011).
- [8] Y.-P. Cai, C.-Y. Su, G.-B. Li, Z.-W. Mao, C. Zhang, A.-W. Xu, B.-S. Kang. *Inorg. Chim. Acta*, **358**, 1298 (2005).
- [9] M. Hakimi, B.-M. Kukovec, M. Minoura. *J. Chem. Crystallogr.*, **42**, 290 (2012).
- [10] (a) H. Eshtiagh-Hosseinia, H. Aghabozorg, M. Shamsipur, M. Mirzaei, M. Ghanbari. *J. Iran. Chem. Soc.*, **8**, 762 (2011); (b) M. Hakimi, K. Moeini, Z. Mardani, E. Schuh, F. Mohr. *J. Coord. Chem.*, **66**, 1129 (2013); (c) Z. Derikvand, G. Bruno, H. Amiri. *Inorg. Chim. Acta*, **410**, 221 (2014); (d) Z. Derikvand, M.M. Olmstead, B.Q. Mercado, A. Shokrollahi, M. Shahryari. *Inorg. Chim. Acta*, **406**, 256 (2013); (e) Z. Derikvand, M.M. Olmstead, A. Shokrollahi, F. Zarghampour. *Synth. React. Inorg. Met-Org. Nano-Met. Chem.*, **45**, 104 (2015); (f) Z. Derikvand, A. Nemati, A. Shokrollahi, F. Zarghampour. *Inorg. Chim. Acta*, **392**, 362 (2012); (g) W.-L. Duan, Y.-H. Zhang, X.-X. Wang, X.-R. Meng. *J. Coord. Chem.*, **67**, 1980 (2014); (h) Q. Huang, W. Tang, C. Liu, X. Su, X. Meng. *J. Coord. Chem.*, **67**, 149 (2014); (i) M.R. Grimmett. *Compr. Heterocycl. Chem.*, **5**, 457 (1984); (j) G. Muller. *Drug Discovery Today*, **8**, 681 (2003).
- [11] H. Aghabozorg, F. Ramezanipour, J. Soleimannejad, M.A. Sharif, A. Shokrollahi, M. Shamsipur, A. Moghimi, J. Attar Gharamaleki, V. Lippolis, A.J. Blake. *Pol. J. Chem.*, **82**, 487 (2008).
- [12] Z. Aghajani, H. Aghabozorg, E. Sadr-Khanlou, A. Shokrollahi, S. Derki, M. Shamsipur. *J. Iran. Chem. Soc.*, **6**, 373 (2009).
- [13] A. Shokrollahi, M. Ghaedi, H.R. Rajabi, M.S. Niband. *Spectrochim. Acta, Part A*, **71**, 655 (2008).
- [14] L. Alderighi, P. Gans, A. Ienco, D. Peters, A. Sabatini, A. Vacca. *Coord. Chem. Rev.*, **184**, 311 (1999).
- [15] P. Gans, A. Sabatini, A. Vacca. *Talanta*, **43**, 1739 (1996).
- [16] H.S. Harned, B.B. Owen, *The Physical Chemistry of Electrolytic Solutions*, 3rd Edn, pp. 634–649, 752, Reinhold Publishing Corp., New York (1958).
- [17] (a) Bruker AXS Inc. *SMART (Version 5.060) and SAINT (Version 6.02)*, Madison, WI, USA (1999); (b) M.C. Burla, R. Caliandro, M. Camalli, B. Carrozzini, G.L. Cascarano, L. De Caro, C. Giacovazzo, G. Polidori,

- R. Spagna. *J. Appl. Cryst.*, **38**, 381 (2005); (c) G.M. Sheldrick. *SHELXL97, Program for Crystal Structure Refinement*, University of Göttingen, Germany (1997); (d) *SHELXT LN, Version 5.10*, Bruker Analytical X-ray Inc., Madison, WI, USA (1998); (e) W. Shi, X.-Y. Chen, B. Zhao, A. Yu, H.-B. Song, P. Cheng, H.-G. Wang, D.-Z. Liao, S.-P. Yan. *Inorg. Chem.*, **45**, 3949 (2006).
- [18] M.V. Kirillova, M.F.C.G. Guedes da Silva, A.M. Kirillov, J.J.R.F. Fraústo da Silva, A.J.L. Pombeiro. *Inorg. Chim. Acta*, **360**, 506 (2007).
- [19] S. Sheshmani, M. Ghadermazi, E. Motieiyani, A. Shokrollahi, Z. Malekhosseini. *J. Coord. Chem.*, **66**, 3949 (2013).
- [20] J.C. MacDonald, T.-J.M. Luo, G. Palmore, R. Palmore. *Cryst. Growth Des.*, **4**, 1203 (2004).
- [21] J.C. MacDonald, P.C. Dorrestein, M.M. Pilley, M.M. Foote, J.L. Lundburg, R.W. Henning, A.J. Schultz, J.L. Manson. *J. Am. Chem. Soc.*, **122**, 11692 (2000).
- [22] H. Aghabozorg, E. Motieiyani, A.R. Salimi, M. Mirzaei, F. Manteghi, A. Shokrollahi, S. Derki, M. Ghadermazi, Sh Sheshmani, H. Eshtiagh-Hosseini. *Polyhedron*, **29**, 1453 (2010).
- [23] G.E. Kirsch, T. Narahashi. *Biophys. J.*, **22**, 507 (1978).
- [24] A. Moghimi, A. Shokrollahi, M. Shamsipur, H. Aghabozorg, M. Ranjbar. *J. Mol. Struct.*, **701**, 49 (2004).
- [25] H. Aghabozorg, J. Attar Gharamaleki, E. Motyeian, M. Ghadermazi. *Acta Crystallogr., Sect. E*, **63**, m2793 (2007).
- [26] K. Kurdziel, T. Głowiak, J. Jezierska. *Polyhedron*, **20**, 3307 (2001).
- [27] B. Barszcz, T. Głowiak, A. Jabłońska-Wawrzycka. *Transition Met. Chem.*, **30**, 221 (2005).
- [28] A. Moghimi, S. Sheshmani, A. Shokrollahi, M. Shamsipur, G. Kickelbick, H. Aghabozorg. *Z. Anorg. Allg. Chem.*, **631**, 160 (2005).
- [29] J.B. English, A.E. Martell, R.J. Motekaitis, I. Murase. *Inorg. Chim. Acta*, **258**, 183 (1997).
- [30] S. Sjöberg. *Acta Chem. Scand.*, **31a**, 718 (1977).
- [31] A. Moghimi, Sh Sheshmani, A. Shokrollahi, H. Aghabozorg, M. Shamsipur, G. Kickelbick, M. Aragoni. *Z. Anorg. Allg. Chem.*, **630**, 617 (2004).
- [32] H. Aghabozorg, E. Motieiyani, A.R. Salimi, M. Mirzaei, F. Manteghi, A. Shokrollahi, S. Derki, M. Ghadermazi, S. Sheshmani. *Polyhedron*, **29**, 1453 (2010).
- [33] Z. Derikvand, N. Dorosti, F. Hassanzadeh, A. Shokrollahi, Z. Mohammadpour, A. Azadbakht. *Polyhedron*, **43**, 140 (2012).
- [34] H. Eshtiagh-Hosseini, H. Aghabozorg, M. Mirzaei, M.M. Amini, Y. Chen, A. Shokrollahi, R. Aghaei. *J. Mol. Struct.*, **973**, 180 (2010).